Structural Engineering and Mechanics, *Vol. 66, No. 5 (2018) 637-648*
DOI: https://doi.org/10.12989/sem.2018.66.5.637

Effects of foundation flexibility on seismic demands of asymmetric buildings subject to near-fault ground motions

Gholam Reza Atefatdoost*[1], Behtash JavidSharifi[2a] and Hamzeh Shakib[3b]

[1]Department of Civil Engineering, Estahban Branch, Islamic Azad University, Estahban, Iran
[2]Fars Regional Electrical Company, Shiraz, Iran
[3]Tarbiat Modares University, Tehran, Iran

(Received September 24, 2017, Revised March 6, 2018, Accepted March 15, 2018)

Abstract. When the centers of mass and stiffness of a building do not coincide, the structure experiences torsional responses. Such systems can consist of the underlying soil and the super-structure. The underlying soil may modify the earthquake input motion and change structural responses. Specific effects of the input motion shall also not be ignored. In this study, seismic demands of asymmetric buildings considering soil-structure interaction (SSI) under near-fault ground motions are evaluated. The building is modeled as an idealized single-story structure. The soil beneath the building is modeled by non-linear finite elements in the two states of loose and dense sands both compared with the fixed-base state. The infinite boundary conditions are modelled using viscous boundary elements. The effects of traditional and yield displacement-based (YDB) approaches of strength and stiffness distributions are considered on seismic demands. In the YDB approach, the stiffness considered in seismic design depends on the strength. The results show that the decrease in the base shear considering soft soil induced SSI when the YDB approach is assumed results only in the center of rigidity to control torsional responses. However, for fixed-base structures and those on dense soils both centers of strength and rigidity are controlling.

Keywords: torsional response; yield displacement-based approach; dynamic soil-structure interaction; strength distribution; stiffness and strength eccentricity

1. Introduction

When excited by lateral ground motions, asymmetric buildings experience irregular coupled translational-torsional responses. Such type of seismic response which may induce a non-uniform inelastic demand through the resisting elements of the structure makes buildings with in-plan non-symmetric strength and stiffness distributions extremely vulnerable to damage under earthquake loads. For this reason, understanding of the seismic torsional behavior of such types of buildings has been the subject of numerous researches (e.g., Aziminejad and Moghadam 2009, Çelebi and Gundez 2005, Hejal and Chopra 1989, Kan and Chopra 1981, Kan and Chopra 1977). In order to mitigate the effects of torsion during earthquake, most seismic codes that provide design guidelines for strength distribution are based on the traditional perception that elements stiffness and strength are independent parameters (Shakib and Atefatdoost 2011). It is assumed in the traditional approach that the stiffness of a Lateral Force Resistant Element (LFRE) can be estimated independently of its strength. As a result of this assumption, stiffness distribution is considered as known prior to allocation of strength. Since stiffness distribution is known, the Center of Rigidity (CR) and the Stiffness Eccentricity, e_R, (defined as the distance between the Center of Mass (CM) and CR) can be readily determined. For this reason, e_R has become a parameter commonly used in torsional provisions. Another approach has been suggested for stiffness-strength dependent LFREs. For an important class of widely used structural elements such as reinforced concrete flexural walls, stiffness is known to be a strength-dependent parameter. This implies that lateral stiffness distribution in a wall-type system cannot be defined prior to assignment of the elements' strength. Therefore, both strength and stiffness eccentricities are important parameters affecting the seismic responses of asymmetric wall-type systems (Mysilmaj and Tso 2004, Mysilmaj and Tso 2002, Tso and Myslimaj 2002, Shakib and Atefatdoost 2011).

Because of deformations within the soil immediately beneath a structure, the motion of the base of a building may differ from that of the ground some distance away. Such a difference is suggestive of soil-structure interaction (SSI). These interactional effects refer to the fact that the dynamic response of a structure built on a site depends not only on the characteristics of the free-field ground motion but also on the inter-relationships of the dynamic structural properties and those of the underlying soil deposits (Wolf 1985, Roy and Sekhar 2010, Sivakumaran *et al.* 1992, Shakib and Atefatdoost 2011). Previous researches have shown that, for a specific structure, the responses during an earthquake may be totally different when the structure is

*Corresponding author, Assistant Professor
E-mail: gh_atefatdoost@iauest.ac.ir
[a]Project superintendent
E-mail: b.javidsharifi@sutech.ac.ir
[b]Professor
E-mail: shakib@modares.ac.ir

http://www.techno-press.com/journals/sem&subpage=7
ISSN: 1225-4568 (Print), 1598-6217 (Online)

founded on deformable soil compared to a fixed-base structure. This difference is due to the fact that SSI may increase the natural periods of the systems, change the system damping due to wave radiation, or modify the effective seismic excitation (Tsicnias and Huchinson 1984, Xu 2006, Rahnema *et al.* 2016, Yang *et al.* 2008). On the other hand, near-fault ground motions have caused high damage to structures situated in the vicinity of seismic sources during recent earthquakes. Compared to far-field ground motions, these motions impose high seismic demands on structures. Near-fault earthquake records have shown to be characterized by a large high-energy pulse. Such impulsive motions cause the fault-normal component to be the main component and to be much more severe than the fault-parallel one. Since such records are unique based on their intrinsic characteristics, vast studies on many different structural systems have been conducted taking into account many different aspects (e.g., Yang *et al.* 2015, Cao *et al.* 2016, Alhan *et al.* 2016, Abdollahzadeh *et al.* 2016, Ke *et al.* 2016, Liu and Zhong 2014, Durucan and Durucan 2016, Ahmadi and Khoshnoudian 2015, Yazdani and Alembagheri 2017). This proves the importance of this factor which shall be addressed more in future researches.

Estimation of the seismic demand of asymmetric buildings involving interdependence of stiffness and strength (e.g., shear walls) without considering SSI has been of attention for many years. The subject of such researches is mainly strength distribution based on the current theory and newer ones such as distribution based on yield displacement (YDB). Also, development of stiffness and strength distribution algorithms, numerically evaluating this algorithm and finding a criterion for the minimum torsional reaction are subjects that have been under investigation (e.g., Mysilmaj and Tso 2004, Myslimaj and Tso 2002, Tso and Myslimaj 2003, Myslimaj and Tso 2001, Mysilmaj and Tso 2004, Shakib and Ghasemi 2007). Several researchers have so far attempted to incorporate the flexibility of foundation in asymmetric system models. Primary researches on this topic have generally been on basic modeling, finding impedance functions, and investigating simple models of such structures in the frequency domain (Balendra *et al.* 1982, Sivakumaran *et al.* 1992, Sivakumaran and Balendra 1994, Tsicnias and Huchinson 1984). Over time, as knowledge over the behavior of asymmetric soil-structure systems increased, and by having faster computers at hand, evaluation of these structural systems became more comprehensive and accurate and thereafter more realistic models have been taken into account considering the non-linear behavior of soil and structure in the time domain. Shakib and Fuladgar (2004) studied the effect of dynamic SSI on the seismic response of asymmetric buildings. An approach was formulated by them for the linear analysis of three-dimensional dynamic SSI of asymmetric buildings in the time domain. They found that the eccentricity ratio of an asymmetric system has a significant effect on the response of the soil-structure system, which is strongly dependent on base flexibility and structural periods. In rather low periods, e.g., $T = 0.5$ as selected in this study, displacements of symmetric buildings situated on very flexible and rather flexible soil conditions are considerably increased by increase of the eccentricity ratio. However, in long structural periods, i.e., T=2 as selected in this study, where the structure is situated on soil conditions similar to the former, lateral displacements are decreased and torsional responses are mildly increased by increase of the eccentricity ratio (Shakib and Fuladgar 2003). A stochastic approach was also adopted by Shakib (2004) for the linear time-domain analysis of three-dimensional dynamic SSI involving asymmetric buildings to evaluate dynamic eccentricity of torsional provisions in seismic building codes. It was concluded that dynamic eccentricity of torsionally coupled flexible-base systems is increased as the base flexibility of the system increases. Nevertheless, by increase of the base flexibility of the system, variations of dynamic eccentricity decrease with respect to static eccentricity. This phenomenon is more evident for systems with higher structural periods (Shakib 2004). Erkan and Necmettin (2005) formulated a simplified methodology of analysis for seismic responses of 3-D irregular high-rise buildings on rigid footings resting on the surface of a linear elastic half-space. They also developed an efficient method in the frequency domain to obtain the structural response of torsionally asymmetric buildings including SSI using modal decomposition. It was concluded that by applying this algorithm, a full advantage is taken of classical normal mode approximation and the interaction problem is solved easily and effectively within the framework of the Fourier-transformed frequency domain analysis for a fixed-base structure (Çelebi and Gundez 2005). Xu (2006) showed that by using this simplified methodology for different numerical studies, both horizontal displacement and rocking of the foundation increase. As a result, the ratio of structure-to-foundation mass and the ratio of structure height to gyration radius will increase (Xu 2006). Jiang, Roy and Chandra (2010) studied inelastic seismic demands of low-rise buildings with soil-flexibility using two types of models: single- and multi-story. In all models, both elasto-plastic and degrading hysteresis behaviors of the lateral load-resisting structural elements were considered, while the sub-soil was idealized as linear and elasto-plastic. It was concluded that the inelastic response of an asymmetric structure relative to its symmetric counterpart is not appreciably influenced due to SSI. The findings also confirmed that the equivalent single-story model, characterized by the lowest period rather than the fundamental period of the real system, tends to yield a conservative estimation of the inelastic demand at least for short-period systems (Roy *et al.* 2010). Chi-Chang *et al.* (2010) tried to analyze SSI effects on vibration control of active tendon systems for torsionally coupled (referred to as TC) structures using a control algorithm along with numerical simulation. The results showed that the effect of SSI on TC structures should be considered in design of active control devices, especially for high-rise asymmetric buildings located on soft site conditions (Lin *et al.* 2010). 3-dimensional models were also studied to fetch results on high torsional responses of structures neglecting foundation flexibility (De-la-Colina 2013). Piles and pile raft effects on asymmetric buildings under earthquake time-history analysis were studied by Brady and Satyam (2015), where

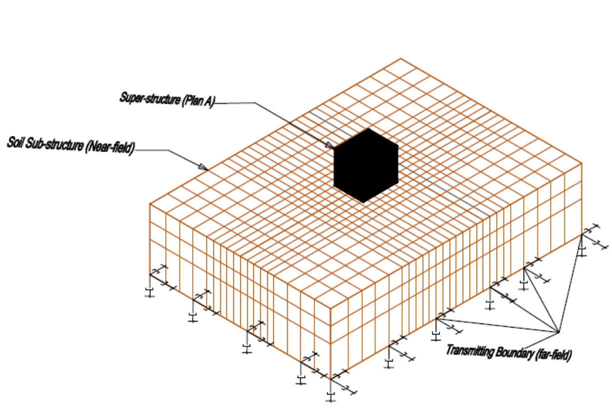

(a) Rigorous model of the soil-structure system

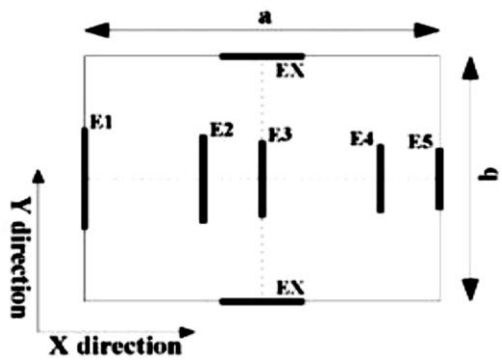

(b) Plan A: Building plan

Fig. 1 Schematic view of the model

Table 1 Characteristics of the shear walls

Wall label	Length (m)	Thickness (m)	Height (m)
E1	3.7	0.30	7.5
E2	3.2	0.30	7.5
E3	2.8	0.30	7.5
E4	2.5	0.30	7.5
E5	2.25	0.30	7.5

2015 Nepal earthquake records were made use of.

The lack of symmetry due to a non-uniform distribution of mass, stiffness or strength is one of the main reasons for occurrence of torsional effects. Moreover, asynchronic movements of the foundation due to characteristics of the seismic excitation lead to torsion in the building. Accordingly, torsion can also happen in symmetric structures. These effects highly depend on foundation type and dimensions of the building compared to the length of the seismic wave (Rosenblueth 1986). In this study, only asymmetric characteristics are considered to account for torsional responses. It is seen in previous researches that in the estimation of seismic demand of asymmetric soil-structure systems, effects of strength distribution based on the interdependence of stiffness and strength and also near-fault motions on this demand have not acquired enough attention. Nonetheless, it seems that both issues are effective on the value and variation of asymmetric structure's seismic demand. In this research, the seismic demands and their variations are considered through numerical approaches for an asymmetric building with reinforced concrete shear walls based on fundamental structural parameters. The two existing points of view, namely the traditional and the yield-displacement based (YDB) in the stiffness and strength distribution and effects of properties of near-fault records are of cases that have been considered. All soil-structure models have been modelled in the time domain through the Finite Element Method and in the framework of OpenSees.

2. Modelling of the soil-structure system

In order to model the soil-structure system to be similar to the one by Shakib (2004), the system shall consist of two main media: a) the super-structure, and b) the sub-structure (the soil system) including near-field and far-field domains. In this study, an idealized asymmetric single-story building resting on homogeneous soil surface is considered (Fig. 1). The geometrical and material properties of the systems are given in Fig. 1.

2.1 Super-structure

The super-structure is composed of a single rectangular uniform slab such that the Center of Mass (CM) is located at the geometric center of the slab which is supported by five reinforced concrete flexural wall elements in the Y-direction. Also, two equal wall elements support the slab at the edges in the X-direction (Fig. 1(b)). The system is assumed to be mono-symmetric. For the sake of numerical inspection, a structure with plan dimensions of $9 \times 12\,m$ and with an effective weight of 126.5 tons is assumed. With respect to the structure's properties, the period is 0.62 and the overall nominal strength is 0.2W, i.e., 25.3 tons (UBC-97). In order to distribute the strength, there are two theories to follow which will be discussed in the following. After assignment of strengths to the walls, all were designed based on ACI-2014.

As was stated earlier, the system was modelled in OpenSees platform. Damping ratio is assumed to be 5% of the critical damping for all models .The diaphragms are assumed to behave rigidly all through the analysis. Hence, the command *rigidDiaphragm* was used for this purpose. In order to model the shear walls, the *NonlinearBeamColumn* element was used which takes into account distributed plasticity through fibers. Concrete characteristic strength and steel yield stress equal 21 MPa and 400 MPa, respectively. Wall properties are given in Table (1). Note that the two walls in the symmetric (i.e., X-) direction are considered to behave only elastically. For the sake of the footing, *ShellMITC*4 elements were used (Mazzoni *et al.* 2007). The foundation thickness is neglected so as to take into account foundation flexibility realistically, and it has the potential to manifest only linear-elastic behavior with a modulus of elasticity equal to that of the constituent concrete (i.e., 2×10^4 MPa).

2.1.1 Strength and stiffness distribution based on the YDB approach

This method of distribution is proposed for structures with LRFE in which stiffness and strength are interdependent. This method has been developed and verified by Priestley and Kowalsky (1998), Mysilmaj and Tso (2001), Mysilmaj and Tso (2002), Mysilmaj and Tso (2004), Mysilmaj and Tso (2004), Tso and Mysilmaj (2003) and Atefatdoost *et al*. (2017). Based on this theory, the yield displacement of each wall is first extracted based on their materials and geometric properties using basic equations such as Eq. (1) (Priestley and Kowalsky 1998)

$$\Delta_y=\left(\frac{2\xi_y h_w^2}{\eta}\right)\frac{1}{l_w} \tag{1}$$

in which l_w and h_w are respectively the length and height of the wall, ξ_y is yield strain of the reinforcing steel and η is a constant equal to 3. For the inspected model, yield displacement values for the five walls (E1 to E5) are calculated respectively to be equal to 1.52, 1.76, 2, 2.24 and 2.48 cm. In the following, fitting a continuous yield distribution function will practically be a basis for strength distribution. Yield displacement approximation of the walls of a story is done using a continuous function. This continuous distribution function can be assumed linear

$$u(x)=\begin{cases}\dfrac{D(1-u_L)}{0.5L+a}x+D & -0.5L-a\le x\le 0\\ \dfrac{D(u_R-1)}{0.5L+b}x+D & 0\le x\le 0.5L+b\end{cases} \tag{2}$$

where D is the yield displacement of the center of mass and is equal to u_L and u_R for the right and left ends of the plan. To calibrate the mentioned linear function, the three values u_L, u_R, and D will suffice. Note that the values of S1 and S2 correspond to the laterally loaded area of elements E_1 and E_n. Lengths a and b are considered to convert the discrete system to a continuous one. Calibration of these parameters is discussed in detail in Atefatdoost *et al.* (2017).

Knowing that one of the main objectives of this algorithm is to distribute strength among the elements, it is next required to well determine a strength distribution function. To achieve this goal, a distribution function similar to that of yield distribution is assumed and shown in Fig. 5. In this continuous function, strength is P in the mass center and is respectively V_L and V_R in the left and right terminal layers. Therefore, the strength distribution function will be of a form as in the following

$$v(x)=\begin{cases}\dfrac{P(1-V_L)}{0.5L+a}x+P & -0.5L-a<x<0\\ \dfrac{P(V_R-1)}{0.5L+b}x+P & 0<x<0.5L+b\end{cases} \tag{3}$$

As in the previous case, the unknowns V_L, V_R and P must be determined. For this purpose, the following assumptions have been considered:

1) Strength eccentricity (e_V) is bound to yield function eccentricity (e_D) with a β factor, as in the following

$$e_V=\beta e_D \tag{4}$$

2) The yield function radius of gyration (r_D) is equal to the strength radius of gyration (r_V)

$$r_D=r_V \tag{5}$$

where β is a key factor in strength and stiffness distribution which imposes the position of strength and stiffness centers. For $\beta > 0$, the strength and stiffness centers are placed on opposite sides of the mass center. By $\beta < 0$ the strength and stiffness centers are on the same side of the mass center. For β =1 the system will lead to small or zero eccentricity and finally β =0 will result in a system with zero strength eccentricity. Calibration of the parameters is discussed in detail in Atefatdoost *et al*. (2017).

After the strength distribution function unknowns are achieved, the form of the function is practically known and can be used to calculate the strength of each element v_i as below

$$v_i=\int_{C_1}^{C_2} v(x)dx \tag{6}$$

where c_1 and c_2 are the top and bottom limits of the integral whose difference states the lateral loaded area of element i (i.e., coordinates of average distances of the walls on each side of the i'th wall). After determining the strength assignment to each LFRE, each stiffness can be eventually calculated using the base equation given in the following

$$K_i=\frac{v_i}{\Delta_{yi}} \tag{7}$$

For the investigated structure, considering the procedure above for distribution of strength and stiffness, the assigned strengths and stiffnesses to the walls are given in Table 2. In a like manner, the locations of centers of strength (e_v) and stiffness (e_k) are calculated and presented in the last two rows of the mentioned table.

2.1.2 Distribution of strength based on the traditional method

In this point of view, stiffnesses of the members are first calculated based on section properties and then, as a basic principle, the strength is distributed among the members proportional to their stiffness. According to this principle, to a stiffer element is assigned a larger strength. This principle is based on the basic assumption that all LRFEs of a story yield together, which can be easily rejected for LRFEs such as shear walls in which yield displacements vary inversely with the wall length as in Eq. (1). Therefore, this method is not thoroughly realistic for concrete structures shear walls (Mysilmaj and Tso 2004, Mysilmaj and Tso 2002, Tso and Myslimaj 2003, Myslimaj and Tso 2001, Mysilmaj and Tso 2004, Priestley and Kowalsky, 1998, Shakib and Ghasemi 2007). The assignments of strength and stiffness to the walls for the investigated asymmetric structure are determined according to Table 3. Note that in this type of assumed distribution, the stiffnesses of the walls are assumed according to the previous section; therefore, β is indirectly imported. The locations of centers of strength (e_v)

Table 2 Strength and stiffness distribution for the set of structures via the YDB approach

Shear wall	β=-0.5	β=-0.25	β=0.0	β=0.25	β=0.50	β=0.75	β=1.0
f_{E1} (ton)	6.45	6.16	5.84	5.52	5.2	4.88	4.56
f_{E2} (ton)	5.43	5.31	5.2	5.08	4.96	4.84	4.72
f_{E3} (ton)	5.23	5.21	5.19	5.17	5.15	5.13	5.11
f_{E4} (ton)	4.19	4.37	4.55	4.73	4.9	5.1	5.27
f_{E5} (ton)	3.98	4.26	4.54	4.82	5.1	5.37	5.65
K_{E1} (kg/cm)	4264	4052	3843	3632	3421	3210	3000
K_{E2} (kg/cm)	3085	3017	2955	2886	2818	2750	2681
K_{E3} (kg/cm)	2615	2605	2595	2585	2575	2565	2555
K_{E4} (kg/cm)	1870	1950	2032	2111	2187	2273	2353
K_{E5} (kg/cm)	1604	1718	1830	1943	2056	2165	2278
e_V (cm)	-36	-18	0	19	36	54	72
e_K (cm)	-109	-92	-75	-57	-39	-21	0

Table 3 Strength and stiffness distribution for the set of structures via the traditional approach

Shear wall	β=-0.5	β=-0.25	β=0.0	β=0.25	β=0.50	β=0.75	β=1.0
f_{E1} (ton)	8.5	8	7.6	7.2	6.9	6.5	6.1
f_{E2} (ton)	6	5.9	5.8	5.7	5.7	5.5	5.5
f_{E3} (ton)	5.1	5.1	5.1	5.1	5.2	5.2	5.2
f_{E4} (ton)	3.7	3.8	4	4.2	4.5	4.6	4.8
f_{E5} (ton)	3.1	3.4	3.6	3.9	4.1	4.5	4.7
K_{E1} (kg/cm)	4263	4052	3842	3631	3421	3210	3000
K_{E2} (kg/cm)	3085	3017	2954	2886	2818	2750	2681
K_{E3} (kg/cm)	2615	2605	2595	2585	2575	2565	2555
K_{E4} (kg/cm)	1870	1950	2031	2111	2187	2272	2352
K_{E5} (kg/cm)	1604	1717	1830	1943	2056	2165	2278
e_V (cm)	-109	-92	-75	-57	-39	-21	0
e_K (cm)	-109	-92	-75	-57	-39	-21	0

and stiffness (e_k) are therein presented in the last two rows of the mentioned table. It is of note that the centers of stiffness and strength coincide based on the traditional view.

2.2 The soil

The soil beneath the structure was divided into two sub-domains, namely the sandy near-field which is the bounded domain of the soil that may exhibit non-linear behavior and the unbounded far-field which extends to infinity. Since the amplitudes of stress decay with respect to the foundation when the distance from the structure increases, non-linearity is assumed to be limited to the bounded soil. The unbounded soil, on the other hand, is assumed to behave only linearly (Wolf 1996, Shakib and Fuladgar 2003, Shakib 2004, Rahnema *et al.* 2016). The bounded soil domain can be modeled with standard finite elements. In this domain, because of the inelastic properties of the soil, non-linear finite elements are used with the UCSD constitutive model which is a pressure dependent model for determining whether or not the material has failed or

Table 4 Suggested values for soil parameters in the UCSD model (Yang *et al.* 2008)

Types Parameters	Type I	Type II
Density (ton/m^3)	1.7	2.1
Reference shear modulus at p_r' = 80 (kPa)	5.5×10^4	1.3×10^5
Reference bulk modulus at p_r' = 80 (kPa)	1.5×10^5	3.9×10^5
Friction angle (degrees)	29	40
Peak shear strain at p_r' = 80 (kPa)	0.1	0.1
Reference pressure (p_r')	80	80
Pressure dependence coefficient	0.5	0.5
Phase transformation angle (degrees)	29	27
Porosity (e)	0.85	0.45

undergone yielding and also to deal with plastic deformations of pressure-dependent materials such as soil (Rahnema *et al.* 2016, Yang *et al.* 2008). Table 4 represents the mechanical properties of the two soil types used as the underlying media of the soil sub-structure in the present study.

A common method for assuming the effect of the unbounded domain is replacing it with transmitting boundary conditions. Lysmer and Kuhlemeyer (1969) proposed the first transmitting boundary idea that is often referred to as viscous boundary condition, which can be modeled with *zeroLength* elements in Opensees. The soil beneath the structure was modelled with solid elements. The typical solid element (*stdBrick* element) has eight nodes with three degrees of freedom at each. The thickness of the underlying soil over the bedrock is assumed to be 30 meters, and the dimensions of the bounded soil is taken to be 150×90 m. The considerable dimensions chosen for the subs-structure make it unnecessary to account for the stiffness of the far-field; hence, suitable implementation of radiation damping on the fictitious boundary shall lead to intended precision. The maximum dimensions of solid elements in the three directions ($\Delta l_{x,y,z}$) is chosen in the following form (Kuhlemeyer and Lysmer 1973, Shakib 2004)

$$\Delta l_{x,y} < {V_s}/{2f_{min}} \tag{8a}$$

$$\Delta l_z < {V_s}/{8f_{min}} \tag{8b}$$

Considering the minimum value of shear wave velocity (for loose sand: V_s = 180 m/sec) along with minimum frequency of the soil-structure system (0.8 Hz), the maximum element dimensions in horizontal and vertical directions will be 115 and 30 meters, respectively (Kuhlemeyer and Lysmer, 1973 and Shakib and Fuladgar, 2003). In the vicinity of the structure and its foundation a finer mesh was utilized with dimensions of 3×3×3 m^3 for the elements, and in the vicinity of the fictitious boundary the dimensions of the brick elements were enough to be taken coarser and equal to 20×20×10 m^3. In order to restrict the separation of the footing from the underlying soil, it shall be enough to bind the degrees of freedom of the

Table 5 Detailed characteristics of the near-fault records

Earthquake	Station	Distance (km)	Component	PGA (g))	PGV (cm/sec)	PGD (cm)	$\frac{\dot{u}_g}{\ddot{u}_g}$	$\frac{u_g}{\dot{u}_g}$	T_p (sec)
Chi-Chi	TCU075	1.5	TCU075-W	0.33	88.2	86.45	0.27	0.98	4.4
			TCU075-N	0.26	38.2	33.24	0.15	0.87	
Gazli	Karakyr	3	GAZ090	0.72	71.6	23.8	0.1	0.33	1.5
			GAZ000	0.61	65.4	25.3	0.11	0.39	
Loma Perita	LGPC16	6.1	LGP000	0.56	94.8	41.2	0.17	0.43	2.3
			LGP090	0.6	51	11.5	0.09	0.23	
Morgan Hfill	Hall Vally	3.4	HVR240	0.31	39.4	7.66	0.13	0.19	1
			HVR150	0.16	12.5	1.84	0.08	0.15	
Loma Perita	Gilory#1	11.2	GO1090	0.47	33.9	8.09	0.07	0.24	0.7
			GO1000	0.41	31.6	6.38	0.08	0.2	
Roodbar	Abbar	24	ABBAR-T	0.51	53	16	0.11	0.3	1.6
			ABBAR-L	0.57	38	11	0.07	0.29	
Naghan	Naghan	5	NAGH -120	0.73	55	8	0.08	0.15	0.7
			NAGH -210	0.52	37	4	0.07	0.11	

Table 6 Eigenvalue analysis of symmetric systems (periods in seconds)

Mode	Fixed	Type-II	Type-I
1	0.63	0.86	1.28
2	0.24	0.49	0.67
3	0.13	0.36	0.49

structural elements on the footing to those on the adjacent soil using the *equalDOF* command. Hence, no intermediary element between the soil and the structure is needed. Trial and error was used to determine the preferable positioning of the fine mesh.

3. Ground motions

In order to investigate the effects of strong ground motions on soil-structure system seismic demands, seven pairs of translational components of near-fault ground motions were selected. Site soil conditions of these records are all S_A as per NEHRP. The characteristics of the records are listed in Table 1.

The main characteristics in choosing these near-fault records included dominancy of peak ground accelerations, velocities, displacements and corresponding spectral quantities in the normal components relative to the parallel components, narrow-bandedness of the normal components and finally observation of a pulse-like motion in the velocity time-history. Note that this pulse-like motion originates from the propagation of rupture-caused wave toward the site with a velocity close to that of the shear wave. This equality of velocities leads to transportation of most of the content of the seismic energy by this pulse. As is common in most researches, pulse period (T_p) is derived from velocity time history (Alavi and Krawinkler 2004, Shakib and Ghasemi 2007). In all models, fault-normal components of earthquakes are exerted to the asymmetric direction of the system while near-fault translational components are simultaneously applied in the perpendicular direction.

4. Results and discussion

In the upcoming sections, a verification of the present models with the fundamental structure is presented and then effects of major structural, soil and earthquake record parameters on seismic demands of asymmetric soil-structure systems are presented.

4.1 Verification

The model was verified to check if it performs agreeably in a soil-structure interactional concept. A free vibration analysis was carried out with symmetric fixed-base condition as well as symmetric structures situated on different soil conditions. The overall geometry, mass and stiffness properties of these structures are equivalent to those of the main models, except that there exists no torsion potential. The periods of the first three modes of vibration for the systems are shown in Table 6. The periods of the symmetric system with Type-II soil are considerably increased compared to those of the fixed-base symmetric system. It is worthwhile mentioning that the increase corresponding to the system including looser sand has been greater than that whose soil has been denser. In addition, non-linear dynamic analyses were carried out on the symmetric fixed-base system as well as on the symmetric soil-structure model with different soil conditions for verification. The variations of normalized non-linear displacement on the time history of the systems subjected to El Centro earthquake record are shown in Fig. 2. Total displacements of the mass centers, i.e. with respect to the bedrock, are recorded. All displacements are divided by the maximum displacement of the fixed-base state. As can be seen in Fig. 2, the normalized non-linear displacement is increased for the symmetric structure on the softer soil. With regard to the performed evaluations, such increases in total displacements and periods are quite logical (Wolf 1985, Shakib and Fuladgar 2003, Roy *et al.* 2010).

4.2 Effects of frequency ratio (Ω)

Effects of the ratio of uncoupled torsional frequency relative to the uncoupled lateral frequency ($\Omega = \frac{\omega_\theta}{\omega_y}$) are verified by evaluating the variations of seismic rotational demand versus β for traditional and YDB approaches of strength distributions and different soil types. Figs. 2 and 3 compare seismic rotational demands of actual and traditionally assumed behaviors of the system subjected to near-fault ground motions. In Fig. 2, for the three support conditions (i.e., two soil conditions along with the fixed-base state) and YDB strength distribution, the seismic rotational demands for different positions of strength and stiffness centers are shown. As seen in all cases, foundation flexibility has a subtractive effect on the rotational demand.

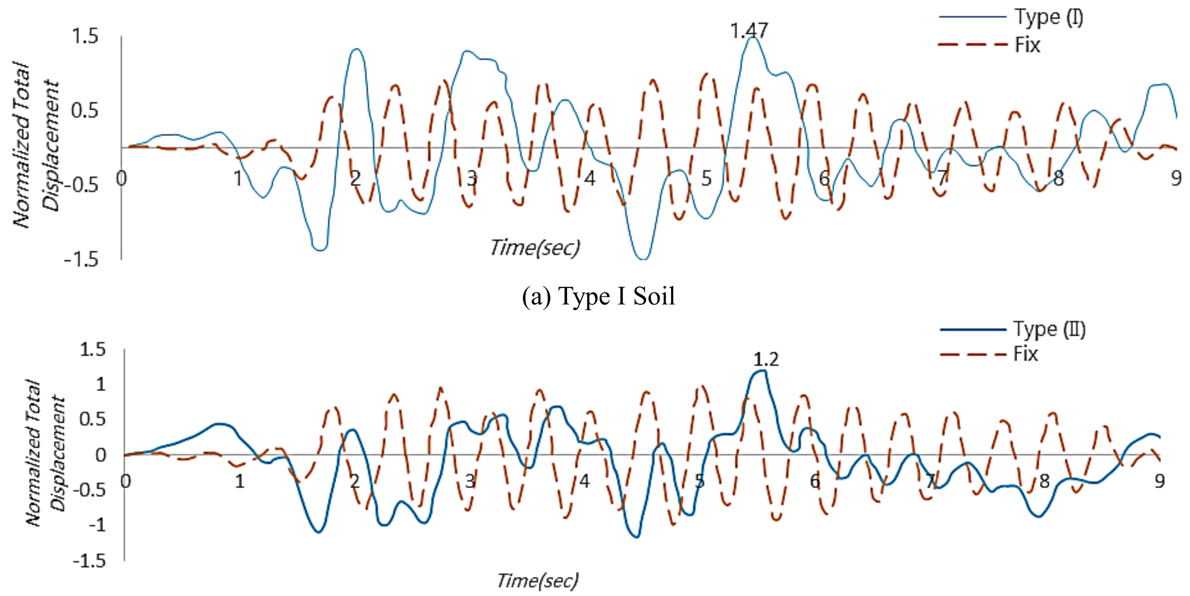

(a) Type I Soil

(b) Type II Soil

Fig. 2 Variation of normalized total displacement response time history of buildings for the two soil conditions subject to El Centro earthquake

For the soft soil condition, rotational responses of the system with Ω = 1 and all β values are maximized. As β increases, for each value of Ω, a decreasing trend is observed. It should be noted that for all ranges of β, Ω = 0.75 renders rotational demands higher than those of Ω =1.5 and 2. Also, for all frequency ratios, the maximum rotational response occurs for the case of β = -0.5 (i.e., maximum stiffness eccentricity), while the minimum response occurs for the case of β = 1 (i.e., minimum stiffness eccentricity). Furthermore, the maximum dispersion of rotational responses happens in the case of β = −0.5 whereas the minimum occurs in the case of β = 1.

For dense soil and fixed-base conditions, the pattern of variations changes significantly compared to the state involving soft soil. As shown in Fig. 2, for β = 0.25 and β = 0.5, rotational responses are almost minimized. Moreover, for β = −0.5 and β = 1, the rotational demands considering different frequency ratios are maximized. It can be concluded that when stiffness and strength centers are located on the same side of the mass center, the rotational response will be maximized. This is while when the stiffness and strength centers are located on opposite sides, the rotational response is minimized. It is of interest that for the fixed-base state similar results have been reported in other previous researches (e.g., Tso and Mysilmaj 2003, Shakib and Ghasemi 2007, Sarvghad and Aziminejad 2009).

Fig. 3 presents the seismic rotational demand versus β-parameter considering the traditional approach and three base conditions. In this case, similar to the YDB approach, foundation flexibility has a subtractive effect on the rotational demand, but patterns of variations of rotation demand in all cases of flexibility are almost similar. As shown in Fig. 3, considering Ω = 1 and for all βs, the rotational demands are maximized. As β increases, for each value of Ω a reducing trend is observed. It should be noted that for all ranges of β, Ω =0.75 takes rotational demands higher than those of Ω =1.5 and 2. For all of the frequency ratios, the maximum rotational response occurs for the case of β = -0.5 (i.e., maximum stiffness eccentricity). This is while the minimum response occurs for the case of β = 1 (i.e., minimum stiffness eccentricity). Furthermore, the maximum dispersion of rotational response happens in the case of β = −0.5 while the minimum occurs in the case of β = 1. It is of interest that for the fixed-base state similar results have been reported by Shakib and Ghasemi (2007).

4.3 Flexibility effects on lateral displacement demand

In order to inspect the effects of fundamental period in the asymmetric direction (T_x), intended periods of 0.5, 1 and 2 seconds were achieved by manipulating the stiffness of the five walls. The manipulations were performed with according variations in yield displacements so as to keep the overall strengths unchanged. The variations of peak relative lateral displacement of CM versus distribution parameter (β) are shown in Figs. 4 to 6, for the mentioned periods, respectively. T_x represents fundamental periods in the X-direction. As can be seen in Fig. 4, for T_x = 0.5 sec in the soft soil condition, the relative lateral displacement response is maximum in β = 1 (i.e., minimum stiffness eccentricity). However, for dense soil and fixed-base conditions, the maximum lateral displacement occurs in β = −0.5. The minimum lateral displacement in all soil conditions occurs in β = 0.5.

Fig. 5 represents the relation between peak displacements and β of SSI for T_x = 1 sec. In this case, for very flexible base systems (i.e., soft soils), lateral displacement is minimum in β = 0.5 and the maximum lateral response occurs in β = 1. It seems that in very flexible base systems, low and medium structural periods have similar patterns in variation of lateral displacement. In

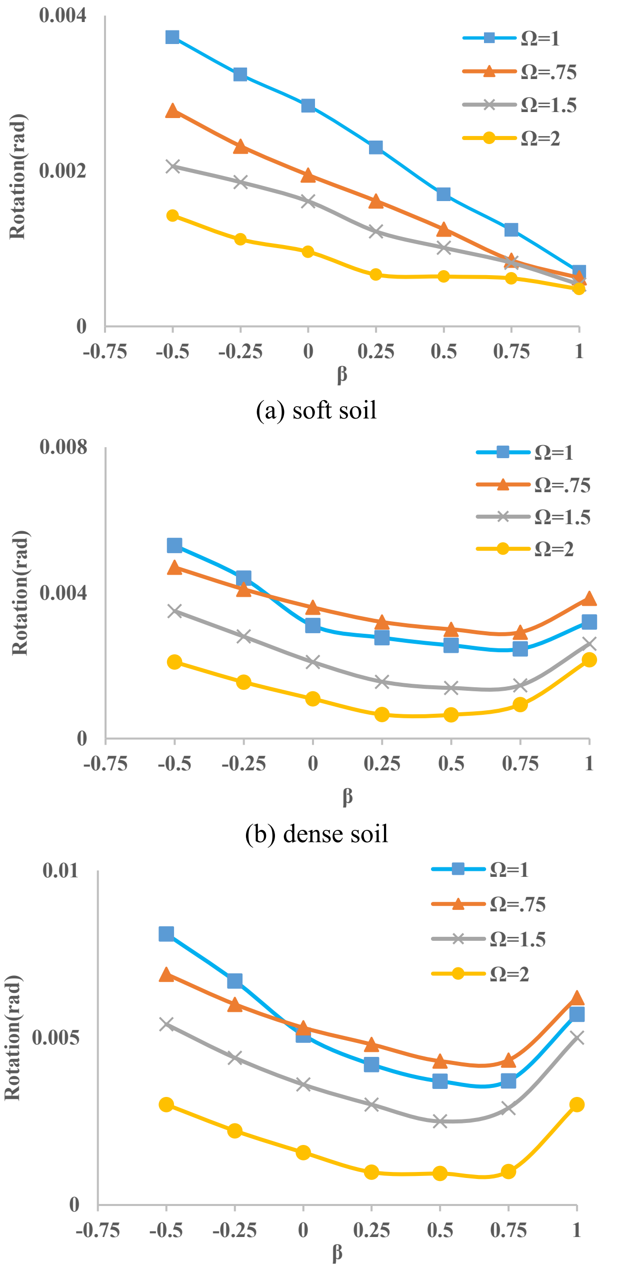

Fig. 2 Comparison of average seismic rotational demands considering the YDB approach for three base conditions

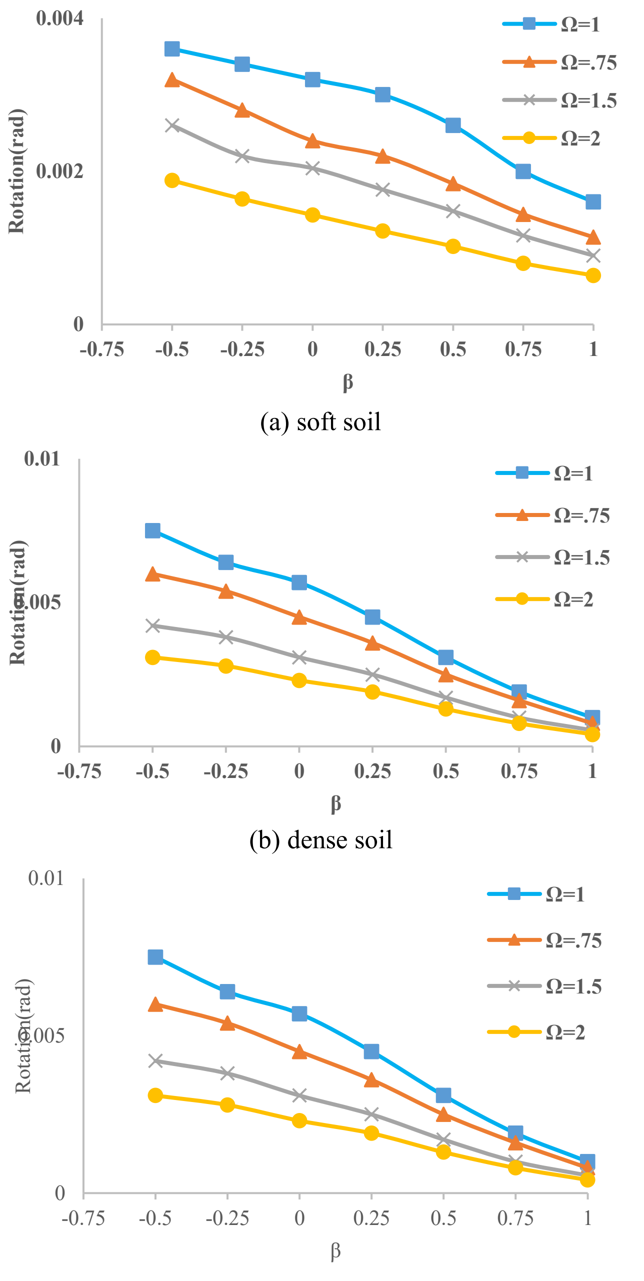

Fig. 3 Comparison of average seismic rotational demands considering the traditional approach for three base conditions

dense soil and fixed-base conditions, the displacement demand is different from that of the soft soil condition. As can be seen in Fig. 5, in these two cases the lateral displacement demand is maximum in $\beta = 1$ (i.e., stiffness eccentricity is minimum) and minimum in $\beta = -0.5$ (i.e., stiffness eccentricity is maximum).

Fig. 6 shows the variations of displacement response for long structural period (i.e., $T_x = 2.0$). As can be seen, for soft soil conditions lateral displacement is maximum in $\beta = 1$ and minimum in $\beta = 0.25$. This is known as the balanced condition. There is a similarity in the pattern of displacement variation for dense soil and fixed-base conditions. In these two cases, the lateral displacement is minimum in $\beta = -0.5$ and maximum in $\beta = 1$.

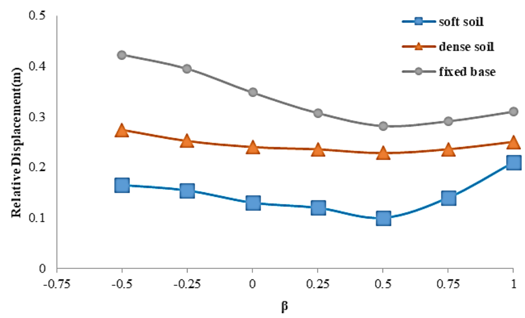

Fig. 4 Variations of average peak lateral displacement of CM versus β for structures with short period (Tx = 0.5 sec) situated on different base conditions

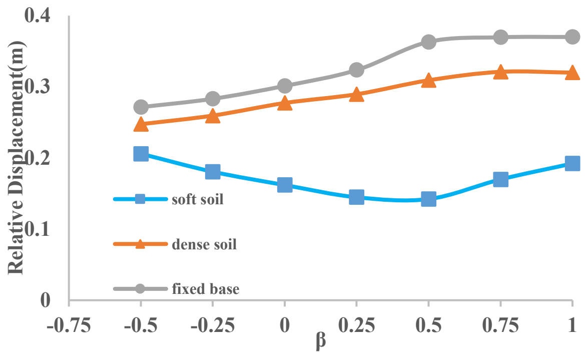

Fig. 5 Variations of average peak lateral displacement of CM versus β for structures with long period (Tx = 1.0) situated on different base conditions

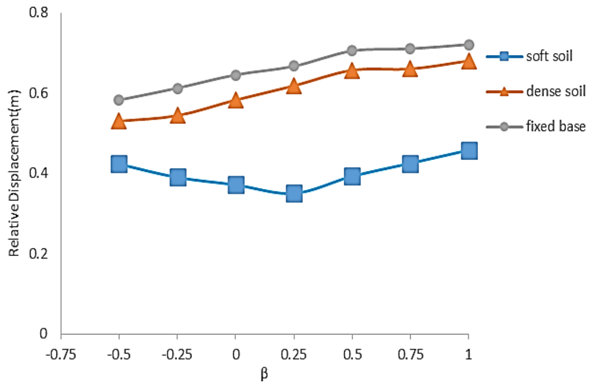

Fig. 6 Variations of average peak lateral displacement of CM versus β for structures with medium period (Tx = 2.0 sec) situated on different base conditions

4.4 Effects on the fundamental structural period

Structural period is an important dynamic characteristic of the structure which considerably influences the dynamic behavior of the system. The fundamental period, i.e., period of the first mode of vibration, has been of interest in this study which is a governing parameter to assess the seismic demands. Fig. 7 presents the maximum floor rotation versus structural period for different values of β parameter as well as different base conditions and periods from 0.5 to 3.0 seconds.

For very flexible conditions, the rotational response gets more considerable as the rigidity of the structure decreases. As can be seen from Fig. 7, for all structural periods considered in this study the rotational response would be minimal when stiffness eccentricity is minimum (β = 1), while the maximum occurs when stiffness eccentricity is maximum. Thus, in soft soil conditions the rotational response of the structure is controlled by stiffness eccentricity. For the dense soil state in the balanced condition for all ranges of periods the torsional response is minimal. This is while in the fixed-base state for short periods the minimum rotational response is similar to that of the medium soil condition that occurs in balanced conditions (i.e., β=0.25 and 0.5), whereas in the long period the minimum rotational response occurs for β = 0.75. On the other hand, for short periods, the minimum rotational response takes place in small strength eccentricities. This is while for long periods this happens in small stiffness eccentricities. It is of interest that for the fixed-base state similar results have been reported by Shakib and Ghasemi (2007).

4.5 Near-fault ground motion pulse period effects

In order to take into account the effects of the pulse-like motion of near-fault records which is of most important characteristics of this type of motion, the parameter T/T_p is addressed. This parameter indicates the ratio of structure's natural period to that of the pulse carried by the motion (Alavi and Krawinkler 2004, Shakib and Ghasemi 2007). Note that the T/T_p parameter is calculated for each motion record per structures' fundamental period. Considering

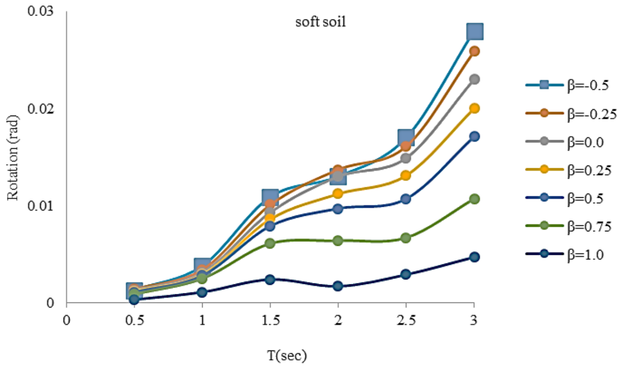

(a) soft soil

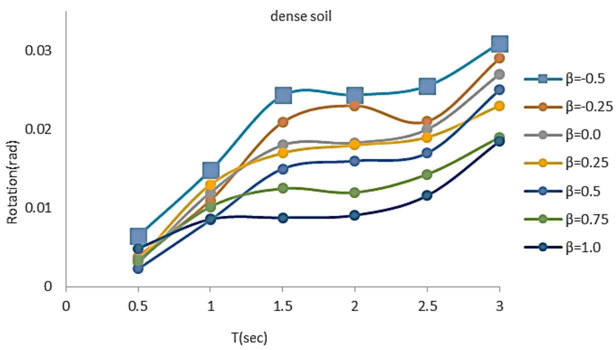

(b) dense soil

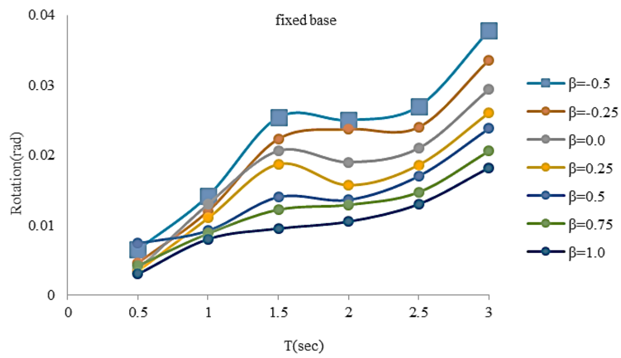

(c) fixed base

Fig. 7 Variations of average seismic rotational demands versus the natural period of buildings situated on different base conditions and β s

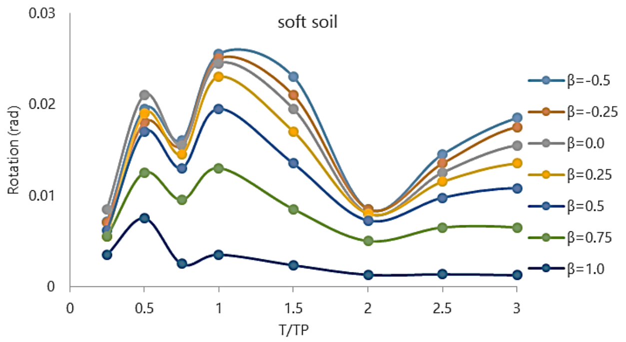

(a) soft soil

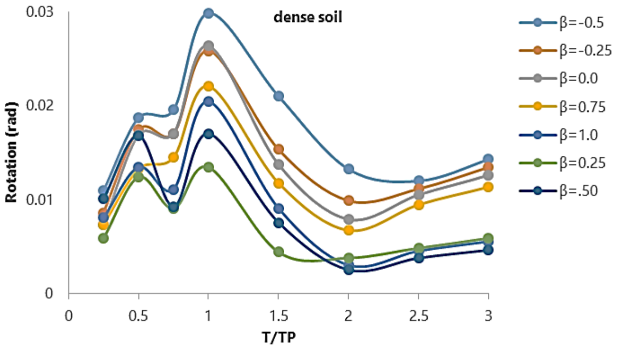

(b) dense soil

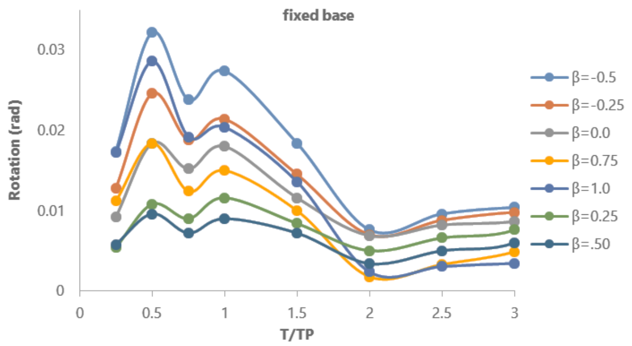

(c) fixed base

Fig. 8 Variations of average seismic rotational demands versus T/T_p for the structure situated on different base conditions and β s

three structural periods of interest in this study and seven records, this will result in 21 T/T_p values for each β. Fig. 8 presents the rotational demand versus T/T_p ratio considering β parameter for three support conditions. It can be seen that in the case of soft soil for $\beta = 1$ minimum rotation and for $\beta = -0.5$ maximum rotation are recorded. Furthermore, rotations corresponding to maximum and minimum stiffness eccentricities ($\beta = 1$ & 0.5) take place at $T/T_p = 1$ and 0.5, respectively. For the cases of dense soil and fixed-base conditions and for all T/T_p, rotations with respect to $\beta = 0.25$ and $\beta = 0.5$ are minimal. However, the maximum rotation for any distribution of strength and stiffness in the fixed-base state takes place when $T/T_p = 0.5$. This is while for dense soil state the same thing goes when $1>T/T_p>0.5$. It is of interest that for the fixed-base state similar results have been reported by Shakib and Ghasemi (2007).

5. Conclusions

Three-dimensional SSI behavior of an asymmetric building under near-fault ground motions was investigated for different positions of stiffness and strength eccentricities. The study findings led to the following conclusions:

1- For buildings situated on different soil conditions assuming the traditional approach, for $\Omega = 1$ and all β values the rotational response would be maximal. Since the major parameter in the mentioned method is stiffness eccentricity, the maximum rotational response occurs in $\beta = -0.5$ while the minimum response is achieved in $\beta = 1$. Also, it is observed that flexibility causes the torsional response to decrease. For soil-structure systems assuming the YDB approach, the maximum torsional response is a function of soil condition. For soft soil conditions, the variation of torsional response is similar to that of the traditional approach so that the maximum torsional response occurs in $\beta = -0.5$ while the minimum is achieved in $\beta = 1$. For both dense soil and fixed-base conditions considering different Ω values, the minimum and maximum rotational demands would occur in $\beta = 0.5$ and $\beta = 1$, respectively.

2- In the YDB approach, the strength distribution ratio (β) of the asymmetric system has a significant effect on the response of the soil-structure system, which is strongly dependent upon base flexibility and structural period of the system. In low-period structures ($T_x = 0.5$), the maximum lateral response for the soft soil condition is in $\beta = 1$, and for dense soil and fixed-base conditions it is achieved in $\beta = -0.5$. In long and medium period structures (i.e., respectively $T_x = 1$ and $T_x = 2$) the maximum lateral response for the soft soil condition is in $\beta = 0.5$ while for the dense soil and fixed-base conditions it is achieved in $\beta = -0.5$. For these systems, maximum lateral responses for any soil condition is in $\beta = 1$.

3- Structural period is another parameter that affects the torsional response of a soil-structure system. This parameter is achieved by changing the structure's stiffness. For very flexible conditions, rotational responses increase as the period of the structure increases. For all structural periods considered in this study, the rotational response would be minimized when stiffness eccentricity is minimum ($\beta = 1$) and the maximum rotational response would occur when stiffness eccentricity is maximum ($\beta = -0.5$). So, in the soft soil condition, the rotational response of the structure is controlled by stiffness eccentricity. For the dense soil condition in all ranges of period, the minimum torsional response is achieved in the balanced condition. In fixed-base and dense soil conditions, the minimum rotational responses for short period occur in $\beta = 0.5$, while for long periods the minimum rotational response happens for $\beta = 0.75$. On the other hand, the minimum rotational response for short period occurs in small strength eccentricity, while for long period it occurs in small stiffness eccentricity.

4- Near-fault ground motion effects were studied using the T/T_P ratio. The rotational response for a soil-structure system can be divided into three regions considering the T/T_p ratio. The maximum rotational response would occur within $T/T_P \leq 1$. However, the rotational demand would be maximum for soft and dense soil conditions exactly in $T/T_P = 1$ and for the fixed-base state in $T/T_P = 0.5$. Within $1 \leq T/T_P \leq 2$, the rotational demand decreases with increase of the T/T_P ratio and for both soil conditions the minimum rotation corresponds to $T/T_P = 2$. Within $T/T_P > 2$, the rotational demand increases with increase of the T/T_P ratio.

References

Ahmadi, E. and Khoshnoudian, F. (2015), "Near-fault effects on strength reduction factors of soil-MDOF structure systems", *Soils Foundat*., **55**(4), 841-856.

Alavi, B. and Krawinkler, H. (2004), "Behavior of moment-resisting frame structures subjected to near-fault ground motions", *Int. J. Earthq. Eng. Struct. Dyn*., **33**(6), 687-706.

Atefatdoost, G.R., Shakib, H. and JavidSharifi, B. (2017), "Distribution of strength and stiffness in asymmetric wall type system buildings considering foundation flexibility", *Struct. Eng. Mech*., **63**(3), 281-292.

Aziminejad, A. and Moghadam, A.S. (2009), "Performance of asymmetric multistory shear buildings with different strength distributions", *J. Appl. Sci*., **9**(6), 1082-1089.

Aziminejad, A. and Moghadam, A.S. (2010), "Fragility-based performance evaluation of asymmetric single-story buildings in near field and far field earthquakes", *J. Earthq. Eng*., **14**(6), 789-816.

Balendra, T., Tat, C.W. and Lee, S.L. (1982), "Modal damping for torsionally coupled buildings on elastic foundation", *Earthq. Eng. Struct. Dyn*., **10**(5), 735-756.

Cengizhan, D. and Ayşe, R.D. (2016), "A_P/V_P specific inelastic displacement ratio for the seismic response estimation of SDOF structures subjected to sequential near fault pulse type ground motion records", *Soil Dyn. Earthq. Eng*., **89**, 163-170.

Cenk, A., Hatice, G. and Hakan, K. (2016), "Significance of stiffening of high damping rubber bearings on the response of base-isolated buildings under near-fault earthquakes", *Mech. Syst. Sign. Proc*., **79**, 297-313.

Chandler, A.M. and Duna, X.N. (1991), "Evaluation of factors influencing the inelastic seismic performance of torsionally asymmetric building", *Earthq. Eng. Struct. Dyn*., **20**(1), 87-95.

Chandler, A.M. and Hutchinson, G.L. (1987), "Code design provisions for torsionally coupled buildings on elastic foundation", *Earthq. Eng. Struct. Dyn*., **15**(4), 517-536.

Chi-Chang, L., Chang-Ching, C. and Jer-Fu, W. (2010), "Active control of irregular buildings considering soil-structure interaction effects", *Soil Dyn. Earthq. Eng*., **30**(3), 98-109.

Chopra, A.K. (1995), *Dynamics of Structures: Theory and Applications to Earthquake Engineering*, Englewood Cliffs, Prentice-Hall, New Jersey, U.S.A.

Dixiong, Y., Changgeng, Z. and Yunhe, L. (2015), "Multifractal characteristic analysis of near-fault earthquake ground motions", *Soil Dyn. Earthq. Eng*., **72**, 12-23.

Erkan, Ç. and Necmetin Gundez, A. (2005), "An efficient seismic procedure analysis for torsionally coupled multistory building including soil-structure interaction", *Turk. J. Eng. Environ. Sci*., **29**(3), 143-157.

Gholamreza, A., Hadi, F. and Hedieh, E. (2016), "Comparing hysteretic energy and inter-story drift in steel frames with V-shaped brace under near and far fault earthquakes", *Alexandr. Eng. J.*

Hejal, R. and Chopra, A.K. (1989), "Earthquake analysis of a class of torsionally coupled buildings", *Earthq. Eng. Struct. Dyn*., **18**(3), 305-323.

Jiang, X.L., Wang, M.L. and Wang, X.Y. (2009), "Analytical model and method of torsionally coupled buildings with foundation interaction", *J. Vibr. Eng*., **22**(5), 546-551.

Kan, C.L. and Chopra, A.K. (1977), "Elastic earthquake analysis of torsionally coupled multi-story buildings", *Earthq. Eng. Struct. Dyn*., **5**(4), 395-412.

Kan, C.L. and Chopra, A.K. (1981), "Simple model for earthquake response studies of torsionally coupled buildings", *ASCE Eng. Mech. Div*., **107**(5), 935-951.

Ke, G.C. and Ke, S. (2016), "Seismic energy factor of self-centering systems subjected to near-fault earthquake ground motions", *Soil Dyn. Earthq. Eng*., **84**, 169-173.

Mazzoni, S., McKenna, F., Scott, M.H. and Fenves, G.L. (2007), *Opensees Command Language Manual of Modeling and Analysis of Structural Systems*.

Myslimaj, B. and Tso, W.K. (2002), "A strength distribution criterion for minimizing torsional response of asymmetric wall-type systems", *Earthq. Eng. Struct. Dyn*., **31**(1), 99-120.

Myslimaj, B. and Tso, W.K. (2005), "A design-oriented approach to strength distribution in single story asymmetric systems with elements having strength-dependent stiffness", *Earthq. Spectr*., **21**(1), 197-221.

Priestley, M.J.N. and Kowalsky, M.J. (1998), "Aspects of drift and ductility capacity of rectangular cantilever structural walls", *Bullet. New Zealand Soc. Earthq. Eng*., **31**(2), 73-85.

Rahnema, H., Mohasseb, S. and JavidSharifi, B. (2016), "2-D soil-structure interaction in time domain by the SBFEM and two non-linear soil models", *Soil Dyn. Earthq. Eng*., **88**, 152-175.

Rana, R., Sekhar, C. and Dutta. (2010), "Inelastic seismic demand of low-rise buildings with soil-flexibility", *Int. J. Non-Lin. Mech*., **45**(4), 419-432.

Rosenblueth, E. (1986), "The 1985 earthquake: Causes and effects in Mexico city", *Concrete Int*., **8**, 23-34.

Shakib, H. (2004), "Evaluation of dynamic eccentricity by considering soil-structure interaction: A proposal for seismic design codes", *Soil Dyn. Earthq. Eng*., **24**(5), 369-378.

Shakib, H. and Atefatdoost, G. (2011), "Effect of soil-structure interaction on torsional response of asymmetric wall type systems", *Proc. Eng*., **14**, 1729-1736.

Shakib, H. and Fuladgar, A. (2003), "Effect of vertical component of earthquake on the response of pure-friction base-isolated asymmetric buildings", *J. Eng. Struct*., **25**(14), 1841-1850.

Shakib, H. and Ghasemi, A. (2007), "Considering different criteria for minimizing torsional response of asymmetric structures under near-fault and far-fault excitations", *Int. J. Civil Eng*., **5**(4), 247-265.

Sivakumaran, K.S. and Balendra, T. (1994), "Seismic analysis of asymmetric multi story buildings including foundation interaction and P effects", *Eng. Struct*., **16**(8), 609-625.

Sivakumaran, K.S., Lin, M.S. and Karasudhi, P. (1992), "Seismic analysis of asymmetric building-foundation systems", *Comput. Struct*., **43**(6), 1091-1103.

Tielin, L. and Wei, Z. (2014), "Earthquake responses of near-fault frame structure clusters due to thrust fault by using flexural wave method and viscoelastic model of earth medium", *Soil Dyn. Earthq. Eng*., **62**, 57-62.

Tsicnias, T.G. and Huchinson, G.L. (1984), "Soil-structure interaction effects on the steady state response for torsionally coupled buildings with foundation interaction", *Earthq. Eng. Struct. Dyn*., **12**(2), 237-262.

Tso, W.K. and Myslimaj, B. (2003), "A yield displacement distribution-based approach for strength assignment to lateral force-resisting elements having strength dependent stiffness", *Earthq. Eng. Struct. Dyn*., **32**(15), 2319-2351.

Wolf, J.P. (1985), *Dynamic Soil-Structure Interaction*, Prentice-Hall Inc., Englewood Cliffs, New Jersey, U.S.A.

Wu, W.H. and Wang, J.F. and Lin, C.C. (2001), "Systematic assessment of irregular building-soil interaction using efficient modal analysis", *Earthq. Eng. Struct. Dyn*., **30**(4), 573-594.

Xu, J.J. (2006), “Simplified analysis procedure for torsionally coupled soil-structure dynamic interaction”, *J. Vibr. Eng.*, **20**(1), 79-84.

Yazdani, Y. and Alembagheri, M. (2017), “Nonlinear seismic response of a gravity dam under near-fault ground motions and equivalent pulses”, *Soil Dyn. Earthq. Eng.*, **92**, 621-632.

Yang, Z., Lu, J. and Elgamal, A. (2008), *OpenSees Soil Models and Solid-Fluid Fully Coupled Elements: User’s Manual*, Version 1. University of California, California, U.S.A.

Yenan, C., Kristel, C.M., George, P.M. and Apostolos, S.P. (2016), “Effects of wave passage on torsional response of symmetric buildings subjected to near-fault pulse-like ground motions”, *Soil Dyn. Earthq. Eng.*, **88**, 109-123.

CC